Intramolecular Electron Transfer between 2,5-Dimethoxy-1,4-phenylene Units in [*n.n*]Paracyclophane Radical Cations

Alexander R. Wartini[a], Jorge Valenzuela[b], Heinz A. Staab[a], and Franz A. Neugebauer*[a]

Arbeitsgruppe Organische Chemie, Max-Planck-Institut für medizinische Forschung[a],
Jahnstraße 29, D-69120 Heidelberg, Germany

Facultad de Ciencias Químicas y Farmacéuticas, Universidad de Chile[b],
Casilla 233, Santiago 1, Chile

Received July 25, 1997

Keywords: Paracyclophanes / Cyclic voltammetry / Radical cations / ESR/ENDOR spectroscopy / Intramolecular electron transfer

A range of [*n.n*]paracyclophane radical cations (**4**$^{\bullet+}$−**12**$^{\bullet+}$), in which two 2,5-dimethoxy-1,4-phenylene units are connected by alkano bridges of varying length, have been studied by ESR and ENDOR spectroscopy. In the [2.2]- and [3.3]paracyclophane radical cations **4**$^{\bullet+}$−**6**$^{\bullet+}$, **10**$^{\bullet+}$ and **11**$^{\bullet+}$ the delocalization of the unpaired electron over both π-moieties and the distinct difference between the first and second oxidation potentials, $\Delta E = E_2^0 - E_1^0$, are evidence for a strong intramolecular electronic interaction between the two electrophores. The [5.5] and [7.7] species (**8**$^{\bullet+}$ and **9**$^{\bullet+}$) are localized radical cations at low temperature (ca. 220 K). At room temperature, the higher molecular flexibility leads to a significant increase in the number of internal collisions between the electrophores, resulting in a fast (ESR time scale) intramolecular electron transfer. The intermediate [4.4]paracyclophane radical cations **7**$^{\bullet+}$ and **12**$^{\bullet+}$ are apparently also localized radical cations. The close interplanar distance between the two π-moieties, however, facilitates their mutual contacts. In **7**$^{\bullet+}$, the intramolecular electron transfer becomes fast on the ESR time scale at room temperature; in **12**$^{\bullet+}$ the transfer is fast over the temperature range 200−300 K.

In [*n.n*]paracyclophanes, two arene units are linked via [*n*]methylene bridges of varying lengths. If $n = 2$, the bridges are rigid; if $n = 3$ or 4, they possess restricted conformational mobility leading to an eclipsed or partially eclipsed arrangement of the linked π-systems. Therefore, [*n.n*]paracyclophanes are attractive model compounds for studying specific intramolecular interactions. Previous investigations of these compounds deal, for example, with the dependence of intramolecular charge transfer on the conformation-related donor-acceptor arrangement[1][2][3][4] or with electron transfer of unsubstituted [*n.n*]paracyclophane radical anions ($n = 2$, 3 and 4)[5] and related radical ions[6]. In these radical ions, the intramolecular ground-state electron exchange between identical π-subunits (electrophores) represents a degenerate process. Depending on the rate of the electron-hopping process, the unpaired electron in the radical ions may be localized on one π-subunit or may be effectively delocalized over both π-subunits within the time scale of the ESR experiment (ca. 10^7 s^{-1}). The rate of the intramolecular electron transfer is mainly influenced by the length and the individual conformation of the alkano bridges and, furthermore, by the reorganization energy, composed of the conformational changes of the molecule upon electron transfer, the rearrangement of the counterion, and the solvent reorganization.

In a fundamental ESR study of [*n.n*]paracyclophane radical anions, Gerson et al.[5] showed that the radical anion of [2.2]paracyclophane (**1**$^{\bullet-}$) generated in dimethoxyethane/hexamethylphosphortriamide (ca. 98:2) is an unassociated species, with the unpaired electron being equally distributed over both π-systems. The same holds for the chair and the boat conformations of the [3.3]paracyclophane radical anion (**2**$^{\bullet-}$), which do not interconvert on the ESR time scale. However, the ESR spectrum of the homologous [4.4]paracyclophane radical anion (**3**$^{\bullet-}$) generated in dimethoxyethane, clearly indicated a localized species. Based on this observation, it was assumed that methylene bridges with $n > 3$ prevent intramolecular electron transfer between the two π-systems. This view is supported by the slow intramolecular electron transfer observed for the 1,2-diphenylethane radical anion[6], and related radical anion systems, e.g. the 1,2-bis(4-nitrophenyl)ethane radical anion[7], 1,2-dianthrylethane and 1,3-dianthrylpropane radical anions[8], and others. For naphthylene moieties connected by rigid bridges, on the other hand, a fast electron exchange in the radical anions was found up to a separation by six C−C single bonds (corresponding to $n = 5$) with intramolecular distances of 7.4[9] and 9 Å[10][11], respectively. Furthermore, Szwarc et al.[12] demonstrated a fast intramolecular electron exchange at higher temperatures for radical anions with two 2-naphthyl units linked by $-(CH_2)_3-$ and $-(CH_2)_4-$ bridges, respectively. These results suggest that in [*n.n*]paracyclophane radical ions with $n > 3$, a fast intramolecular electron exchange might also occur via folded conformations with more proximal electrophores. The observation of the localized **3**$^{\bullet-}$ in dimethoxyethane at low temperature

  1434−193X/98/0101−0139 $ 17.50+.50/0

could be merely a result of the restricted experimental conditions, which favor ion pairing.

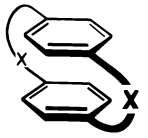

	X
1	$-(CH_2)_2-$
2	$-(CH_2)_3-$
3	$-(CH_2)_4-$

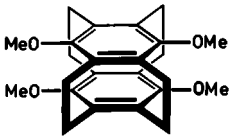

4

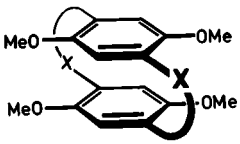

	X
5	$-(CH_2)_2-$
5a	5,8-D_2 $-(CH_2)_2-$
6	$-(CH_2)_3-$
7	$-(CH_2)_4-$
8	$-(CH_2)_5-$
9	$-(CH_2)_3-CO-(CH_2)_3-$

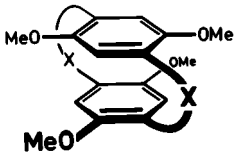

	X
10	$-(CH_2)_2-$
10a	5,8-D_2 $-(CH_2)_2-$
11	$-(CH_2)_3-$
12	$-(CH_2)_4-$

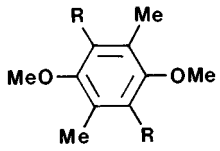

	R
13	H
14	Me

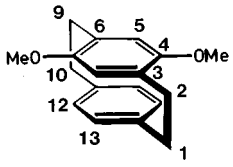

15	
15a	1,1,10,10,12,13,15,16-D_8
15b	1,1,2,2,9,9,10,10,12,13,15,16-D_{12}

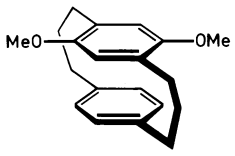

16

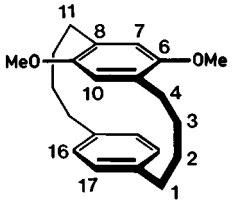

17

Since the features of intramolecular electron transfer in larger [*n.n*]paracyclophane radical ions ($n > 3$) are not yet clearly characterized, we studied a range of radical cations generated from paracyclophanes with 2,5-dimethoxy-1,4-phenylene electrophores (**4**$^{\bullet+}$−**12**$^{\bullet+}$), which have the advantage that ion pairing is less significant. They are also more persistent and allow ESR measurements to be made up to room temperature.

Further information on the intramolecular electron interaction, and hence the electron transfer rate, can be obtained by cyclic voltammetric studies. For compounds consisting of two identical arene electrophores linked by varied alkano bridges, for example, the limit of the fast intramolecular electron transfer in the derived radical anions was found to correspond to a difference of 0.1 V between the first and second reduction potentials, $E_2^0 - E_1^0 \approx -0.1$ V[8]. A similar value was observed for 1,4,8,11-pentacenetetrone radical anions ($E_2^0 - E_1^0 \approx -0.2$ V), supposed to represent a conjugated two-electrophore system with the unpaired electron being localized in a naphthoquinoid unit[13]. Based on these findings, one can assume that in comparable molecular systems a difference of larger than 0.2 V between the first and second redox potentials points to a fast intramolecular electron transfer on the ESR time scale. Therefore, we determined the oxidation potentials of **4**−**12** by cyclic voltammetry in order to get a more detailed picture of the intramolecular electronic interaction in these compounds.

Cyclic Voltammetric Measurements

Table 1 gives the oxidation potentials of the [*n.n*]paracyclophanes **4**−**12** and **15**−**17**, together with those of the reference compounds **13** and **14**. The oxidation potentials were measured in acetonitrile/0.1 M tetrabutylammonium hexafluorophosphate versus Ag/AgCl using a glassy carbon electrode. All data are referred to ferrocene; the oxidation potential $FeCp_2^{+/0}$ was set to 0.00 V. Cyclic voltammetry verified all the compounds to be distinct electron donors.

Table 1. Oxidation potentials and potential differences, $\Delta E = E_2^0 - E_1^0$, of the compounds **4**-**17** in acetonitrile/0.1 M tetrabutylammonium hexafluorophosphate[a]; the oxidation potentials E^0 are given versus ferrocene $FeCp_2^{+/0}$

	E_1^0(± 0.01)/V	E_2^0(± 0.01)/V	$\Delta E = E_2^0 - E_1^0$/V
4	+0.56	+0.76	0.20
5[14]	+0.34	+0.69	0.35
6[14]	+0.33	+0.67	0.34
7	+0.59	+0.80	0.21
8	+0.65	+0.73	0.08
9	+0.71	–	–
10[14]	+0.48	+0.77	0.29
11[14]	+0.47	+0.83	0.36
12	+0.60	+0.81	0.21
13[14]	+0.68	–	–
14	+0.99	–	–
15[14]	+0.49	–	–
16	+0.48	–	–
17	+0.61	–	–

[a] Glassy carbon electrode versus Ag/AgCl; reference ferrocene ($E_1^0 = 0.352$ V) set to 0.00 V.

In their cyclic voltammograms, the [*n.n*]paracyclophanes with one 2,5-dimethoxy-1,4-phenylene moiety (**15-17**) show one reversible one-electron oxidation step, like the reference compound 1,4-dimethyl-2,5-dimethoxybenzene (**13**). The linked 1,4-phenylene moiety in **15-17** operates as an additional donor electrophore. Owing to significant intramolecular interaction between the two π-systems, the oxidation potentials of **15** ($n = 2$, $E_1^0 = +0.49$ V) and of **16** ($n = 3$, $E_1^0 = +0.48$ V) are markedly lower than that of the reference compound **13** ($E_1^0 = +0.68$ V). With further extension of the methylene bridges, the intramolecular interaction decreases considerably, but is still present in **17** ($n = 4$, $E_1^0 = +0.61$ V), as indicated by the relative potential difference between **13** and **17**: E_1^0 (**13**) − E_1^0 (**17**) = +0.07 V.

The cyclic voltammograms of **4**-**7** and **10**-**12** show two distinctly separated and reversible one-electron oxidation steps. Typical examples are the cyclic voltammograms of **6** and **7**, as shown in Figure 1. Owing to the intramolecular electronic interaction between the electrophores, the first oxidation potentials of these cyclophanes are lower than that of the reference compound **13**. Furthermore, in both the *pseudogeminal* (**5**, **6**) and the *pseudoortho* series (**10**, **11**), the first and second oxidation potentials of the corresponding [2.2]- and [3.3]paracyclophanes are very similar, indicating virtually uniform intramolecular π-π interactions. This is probably the result of comparable short transannular distances between the π-moieties in these compounds, which is confirmed by their crystal structure determinations; in **5**: 3.07[15] and **6**: 3.32 Å[2b], and in **10**: 3.05[15] and **11** 3.25 Å[2b], respectively. The minor but clearly evident deviations in the oxidation potentials of the *pseudogeminal* paracyclophanes **5** and **6** ($E_1^0 \approx +0.34$, $E_2^0 \approx +0.68$ V) as compared to those of the *pseudoortho* ones **10** and **11** ($E_1^0 \approx +0.48$, $E_2^0 \approx +0.80$V) are caused by the different mutual orientation of the electrophores. Previous studies of charge-transfer interactions in related quinhydrones have proved that the *pseudogeminal* arrangement with better suited π-overlap favors the intramolecular interaction between the π-moieties[1][2].

Figure 1. Cyclic voltammograms of **6**, **7** and **8** in acetonitrile/0.1 M tetrabutylammonium hexafluorophosphate, $v = 100$ mV s^{-1}

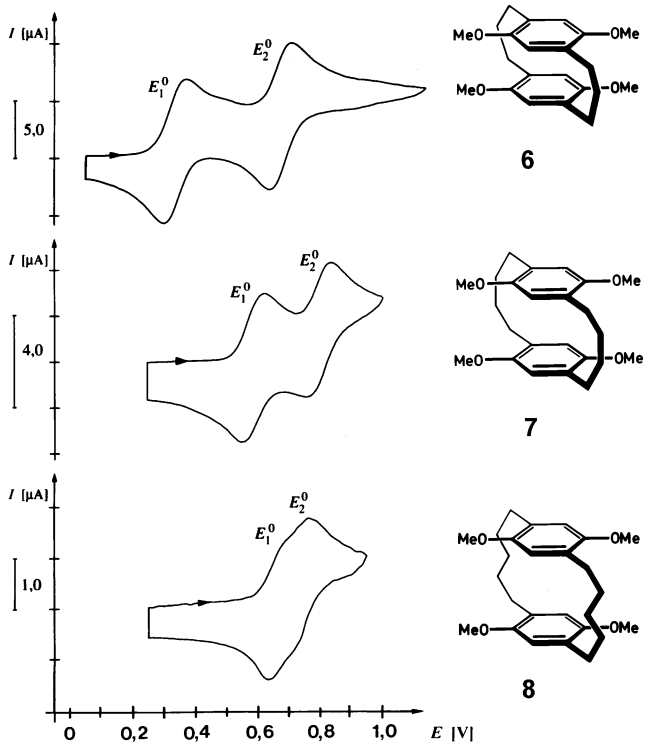

The oxidation potentials of **4** ($E_1^0 = +0.56$, $E_2^0 = +0.76$ V) and its reference compound **14** ($E_1^0 = +0.99$ V) are distinctly higher than those of **5** ($E_1^0 = +0.34$, $E_2^0 = +0.69$ V) and **13** ($E_1^0 = +0.68$ V), indicating that **5** and **13** are stronger electron donors. Clearly, the four space-demanding methyl groups in **14** and the fourfold ethano bridges in **4** preclude a coplanar arrangement of the methoxy substituents with respect to the central π-system, thus considerably reducing their mutual electronic interaction, particularly in the corresponding radical cations.

Further extension of the bridges leads to a marked increase in the separation of the electrophores. According to crystal-structure determinations, the interplanar distances of the *pseudogeminal* **7** ($n = 4$)[3] and **8** ($n = 5$)[4] are 4.01 and 5.11 Å, respectively. This increased separation of the electrophores significantly reduces their intramolecular interaction. In the cyclic voltammogram of **7**, the two reversible one-electron oxidation steps are still clearly resolved (Figure 1), the small intramolecular electronic interaction, however, facilitates the first oxidation only slightly (+0.59 V, cf. reference compound **13** +0.68 V), and the potential difference, $\Delta E = E_2^0 - E_1^0$ is reduced to 0.21 V. This effect is even more pronounced in the cyclic voltammogram of **8**, which shows two very weakly indicated one-electron oxidation steps yielding a potential difference of $E_2^0 - E_1^0 = +0.08$ V (Figure 1). In the further extended paracyclophane **9**, the interplanar distance between the electrophores in the crystal structure increases to 7.38 Å[16]. Its cyclic voltammogram shows one oxidation wave with the normal shape of a one-electron transfer step at 0.71 V, similar to that of the reference compound **13** (+0.68 V). This implies that the first and the second electron transfers occur at the same potential and the two electrophores of **9** can be considered as being almost independent. The potential differences measured, $\Delta E = E_2^0 - E_1^0$, suggest that the limit of a fast electron exchange with regard to the ESR time scale probably lies in the range of the [4.4]- (**7**: $\Delta E = +0.21$ V; **12**: $\Delta E = +0.21$ V) and [5.5]paracyclophane radical cations (**8**: $\Delta E = +0.08$ V).

ESR and ENDOR Studies

Owing to the low-lying first oxidation potential, radical cations are readily formed by oxidation of the parent compounds with lead tetraacetate in trifluoroacetic acid and in dichloromethane/trifluoroacetic acid (99:1), respectively. The ESR and ENDOR results, i.e. the isotropic hyperfine coupling (HFC) constants of all the studied radical cations are collected in Table 2.

The resolved ESR spectrum of the basic reference radical cation **13**$^{\bullet+}$ was well simulated with the values given inTable 2, which are close to the reported data[17] determined under other experimental conditions. In addition, general triple resonance[18] provided the relative signs of the ^{1}H-HFC constants. As one would expect, positive values were found for the two sets of methyl hydrogen atoms and a negative value for the ring hydrogen atoms. The second reference species, the 4,7-dimethoxy[2.2]paracyclophane radical cation (**15**$^{\bullet+}$), afforded a highly resolved ESR spectrum (linewidth ca. 60 mG) with a very complex hyperfine structure, which could only be partially analyzed in combination with ESR and ENDOR results obtained from selectively deuterated derivatives. In the radical cation **15b**$^{\bullet+}$, all hydrogen atoms of the 1,4-phenylene moiety and of the ethano

Table 2. Isotropic hyperfine coupling constants of the radical cations **4**$^{\bullet+}$, **5**$^{\bullet+}$, **7**$^{\bullet+}$–**10**$^{\bullet+}$, **12**$^{\bullet+}$, **13**$^{\bullet+}$, **15**$^{\bullet+}$, and **17**$^{\bullet+}$, in trifluoroacetic acid unless otherwise stated, and *g* values

	Method	*T*/K	a(H−OCH_3)/G	a($H_{aromatic}$)/G	a(H)/G	a(H)/G	a(H)/G	a(H)/G	*g*
4$^{\bullet+}$	ESR	270	1.19 (12 H)	–	0.57 (8 H)	0.04 (8 H)	–	–	2.0033
	ENDOR	270	+1.20	–	+0.58	+0.04	–	–	–
5$^{\bullet+}$	ESR	293	1.37 (12 H)	0.67 (4 H)	0.24 (4 H)	0.21 (4 H)	–	–	2.0032
	ENDOR	270	+1.38	−0.67[a]	+0.22	+0.18	–	–	–
7$^{\bullet+}$	ESR[b]	320	1.46 (12 H)	–	1.46 (4 H)	–	–	–	2.0034
	ESR[b]	170	2.63 (6 H)	–	2.63 (2 H)	–	–	–	–
	ENDOR[b]	190	+2.48	−0.20	+2.79	+0.90	+0.65	–	–
8$^{\bullet+}$	ESR	340	1.50 (12 H)	–	1.50 (4 H)	–	–	–	2.0035
	ESR	260	2.66 (6 H)	–	3.30 (2 H)	–	–	–	–
	ESR[b]	180	3.10 (6 H)	–	4.50 (2 H)	–	–	–	–
9$^{\bullet+}$	ESR[b]	290	1.50 (12 H)	–	1.50 (4 H)	–	–	–	–
	ESR[b]	220	3.05 (6 H)	–	4.13 (2 H)		–	–	2.0035
	ENDOR[b]	190	3.25	–	3.25		–	–	–
10$^{\bullet+}$	ESR	295	1.37 (12 H)	0.72 (4 H)	1.14 (4 H)	0.32 (4 H)	–	–	2.0033
	ENDOR	270	+1.37	−0.73[c]	+1.15	+0.30	–	–	–
12$^{\bullet+}$	ENDOR	295	+1.52	−0.30	+1.79	+0.55	–	–	2.0035
	ENDOR	265	+1.53	−0.31	+1.77	+0.55	–	–	–
	ENDOR[b]	240	+1.54	−0.34	+1.77	+0.55	–	–	–
	ENDOR[b]	180	+1.54	−0.35	+1.72	+0.56	–	–	–
13$^{\bullet+}$	ESR[d]	300	3.19 (6 H)	0.49 (3,6-H)	4.45 (6 H, CH_3)		–	–	2.0035
	ESR	293	3.13 (6 H)	0.46 (3,6-H)	4.45 (6 H, CH_3)		–	–	2.0035
	ENDOR	270	+3.13	−0.47	+4.43		–	–	–
15$^{\bullet+}$	ESR	293	2.76 (6 H)	0.83 (5,8-H)	2.33 (2,9-H)	0.95 (2′,9′-H)	–	–	2.0035
	ENDOR	270	+2.77	−0.83	+2.35	+1.02	[e]	–	–
15a$^{\bullet+}$	ESR	293	2.75 (6 H)	0.85 (5,8-H)	2.35 (2,9-H)	1.09 (2′,9′-H)	–	–	–
	ENDOR	270	+2.76	−0.84	+2.35	+1.04	–	–	–
15b$^{\bullet+}$	ENDOR	270	+2.77	−0.83	–		–	–	–
17$^{\bullet+}$	ESR	265	3.18 (6 H)	–	3.18 (2,9-H)		–	–	2.0035
	ENDOR	265	+3.06	−0.53	+3.48	+0.98	[f]	–	–
	ENDOR[b]	220	+3.12	−0.56	+3.45	+1.04	+0.77	0.21	–

[a] In the special triple-resonance spectrum of **5a**$^{\bullet+}$ the intensity of the 0.95-MHz signal pair is reduced by ca. 50% compared to that of **5**$^{\bullet+}$. – [b] In dichloromethane/trifluoroacetic acid (99:1). – [c] In the special triple-resonance spectrum of **10a**$^{\bullet+}$ the intensity of the 1.03 MHz signal pair is reduced by ca. 50% compared to that of **10**$^{\bullet+}$. – [d] In sulfuric acid[17]. – [e] Three additional line pairs were observed corresponding to a(H) = −0.57, a(H) = −0.39 and a(H) = −0.14 G. – [f] Two additional line pairs were observed corresponding to a(H) = +0.20 and a(H) = 0.09 G.

bridges are replaced by deuterium. The ^{1}H ENDOR of **15b**$^{\bullet+}$ shows two line pairs corresponding to a(H-OCH_3, 6 H) = +2.77 and a(5,8-H) = −0.83 G. Their assignment is based on the hyperfine structure of the ESR spectrum. For the less deuterated **15a**$^{\bullet+}$, two further ^{1}H splittings are expected, representing the two sets of the 2,9-methylene hydrogen atoms, arranged *syn* or *anti* with regard to the methoxy substituents. In fact, both coupling constants are found in the ESR and ENDOR spectra of **15b**$^{\bullet+}$; ENDOR: a(2,9-H) = +2.35 and a(2′,9′-H) = +1.04 G. An unambiguous assignment of these coupling constants to the specific *syn* and *anti* positions of the methylene hydrogen atoms is not yet possible. Besides these major HFS coupling constants, the ENDOR spectrum of the non-deuterated **15**$^{\bullet+}$ shows three additional line pairs corresponding to a(H) = -0.57, a(H) = −0.39, and a(H) = −0.14 G, which originate from the four remaining hydrogen sets (1,10-H, 1′,10′-H, 12,15-H and 13,16-H). With the present experimental results, these additional splittings cannot be assigned to individual hydrogen sets. Based on the results of **15**$^{\bullet+}$, the ESR and ENDOR spectra of the third reference compound, the 6,9-dimethoxy[4.4]paracyclophane radical cation (**17**$^{\bullet+}$), were analyzed yielding the major coupling constants (ENDOR 265 K): a(H-OCH_3, 6H) = +3.06, a(4,11-H) = +3.48 and a(4′,11′-H) = +0.98, and a(7,10-H) = −0.53 G. The apparent changes in the magnitudes of the splittings as compared to the data of **15**$^{\bullet+}$ indicate the release of molecular strain when the bridges are lengthened. Particularly, the increase of the larger methylene hydrogen coupling constant [**15**$^{\bullet+}$: a(2,9-H) = +2.35; **17**$^{\bullet+}$: a(4,11-H) = +3.48 G] clearly indicates a marked decrease of the dihedral angle θ, i.e. the relative orientation of the β-C-H bond with regard to the axis of the adjacent π(2*p*)-orbital.

In the fourfold bridged radical cation **4**$^{\bullet+}$, the close spatial arrangement of the electrophores leads to a symmetrical delocalization of the unpaired electron over the whole molecule. The ENDOR spectrum of **4**$^{\bullet+}$ shows three line pairs (Figure 2), originating from the OCH_3 hydrogen atoms (12 H) and the methylene hydrogen atoms located *syn* (8 H) and *anti* (8 H) with regard to the OCH_3 substituents. General triple resonance (Figure 2) indicates that all three splittings have the same sign (+). Based on the simulation of the well-resolved ESR spectrum (linewidth ca. 20 mG), the largest splitting (1.19 G) has to be assigned to the OCH_3 hydrogen atoms (12 H). The methylene hydrogen splittings are small, since these hydrogen atoms lie close to the nodal plane of the π-moieties. As expected, the a(H-OCH_3) splitting of **4**$^{\bullet+}$ is of about half the magnitude (1.19 G) compared with the a(H-OCH_3) splitting of the corresponding reference radical cation **14**$^{\bullet+}$ [a(H-OCH_3) = 2.76 G[19]]. In

both species, the complete substitution with methyl groups or ethano bridges prevents a coplanar arrangement of the methoxy substituents with regard to the π-plane. Therefore, the a(H-OCH_3) splittings of $\mathbf{4}^{\bullet+}$ and $\mathbf{14}^{\bullet+}$ are smaller than the corresponding values of $\mathbf{5}^{\bullet+}$, $\mathbf{10}^{\bullet+}$ and $\mathbf{13}^{\bullet+}$ (Table 2), which have less steric restrictions.

Figure 2. ^{1}H-ENDOR spectrum of the radical cation $\mathbf{4}^{\bullet+}$ in trifluoroacetic acid at 270 K together with a general triple-resonance spectrum, pump frequency 12.59 MHz

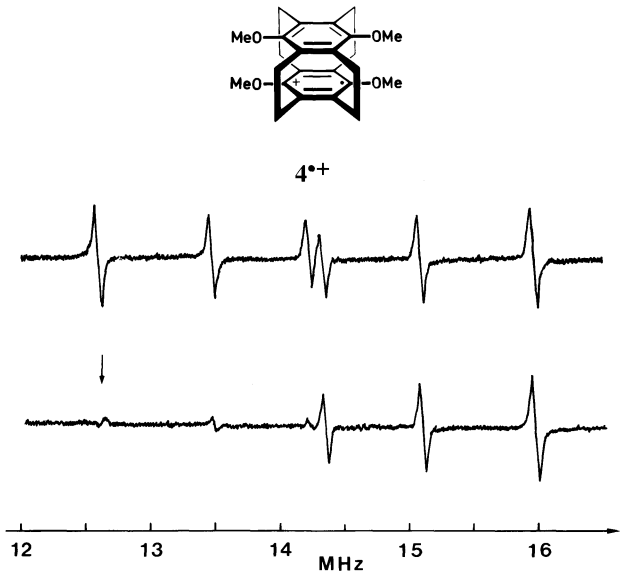

The ESR spectrum of the *pseudogeminal* radical cation $\mathbf{5}^{\bullet+}$ (Figure 3) was well simulated with the coupling constants evaluated from the four line pairs in the ENDOR spectrum. The largest value, a(H) = +1.37 G, can be straightforwardly assigned to the twelve methoxy hydrogen atoms. Also clear is the assignment of a(H) = −0.67 G to the ring hydrogen atoms (5,8,13,16-H), supported by its sign and confirmed by partial deuteration at these positions ($\mathbf{5a}^{\bullet+}$). The remaining two splittings, a(H) = +0.24 (4 H) and a(H) = +0.21 G (4 H), represent the two sets of *syn* and *anti* methylene hydrogen atoms, which cannot yet be specifically assigned. Similar results were obtained for the corresponding *pseudoortho* radical $\mathbf{10}^{\bullet+}$. The highly resolved ESR spectrum (Figure 4) was well fitted using the values given in Table 2. The assignment of a(H-OCH_3) = +1.37 and a(5,8,13,16-H) = −0.72 G also follows from the simulation of the ESR spectrum and the results obtained for the partially deuterated $\mathbf{10a}^{\bullet+}$. Surprisingly, one of the methylene hydrogen coupling constants of the *pseudoortho* $\mathbf{10}^{\bullet+}$ turns out to be distinctly larger [a(H) = + 1.14 G] than that of the *pseudogeminal* isomer $\mathbf{5}^{\bullet+}$ [a(H) = + 0.24 or 0.21 G]. Since there are no significant differences in the strained molecular frameworks of **5** and **10** (the interplanar distances are similar, 3.07 and 3.05 Å, respectively), the large methylene hydrogen splitting of $\mathbf{10}^{\bullet+}$ may be related to a specific through-space interaction. Any further discussion, however, requires an unambiguous assignment of this splitting to the *syn* or *anti* set of the methylene hydrogen atoms. At this stage, however, we see no way of achieving such an assignment. As already verified for a range of [2.2]cyclophane radical ions[6], the results with $\mathbf{4}^{\bullet+}$, $\mathbf{5}^{\bullet+}$ and $\mathbf{10}^{\bullet+}$ prove that the unpaired electron is delocalized over the whole molecule on the ESR time scale. Owing to the large intramolecular electronic interaction between the two π-systems, these radical cations can be considered as being delocalized species.

Figure 3. ESR spectrum of the radical cation $\mathbf{5}^{\bullet+}$ in trifluoroacetic acid at 293 K together with a simulation using the data in Table 2

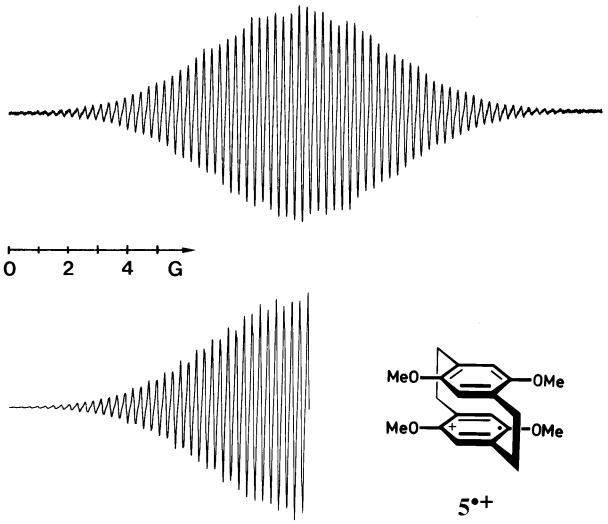

Figure 4. Low-field half of the ESR spectrum of the radical cation $\mathbf{10}^{\bullet+}$ in trifluoroacetic acid at 295 K together with a simulation using the data in Table 2

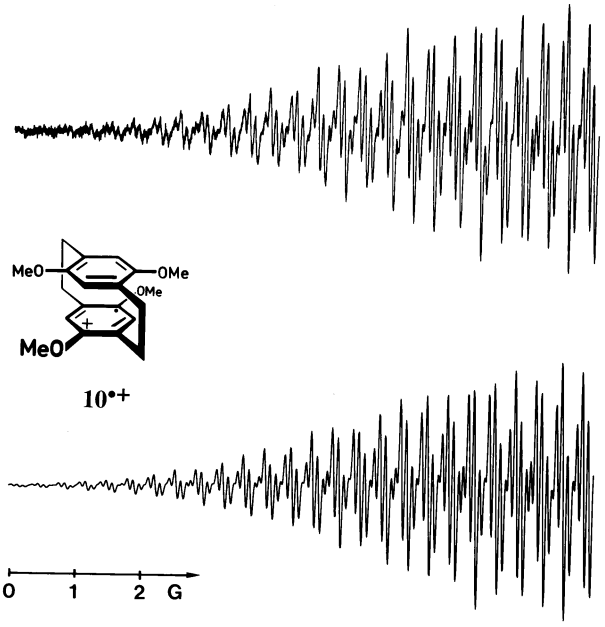

[3.3]Paracyclophanes exist in solution as chair and boat conformers. The barrier of their interconversion lies in the range 10-12 kcal/mol according to dynamic ^{1}H-NMR investigations[20]. Tentative studies of the radical cations $\mathbf{6}^{\bullet+}$, $\mathbf{11}^{\bullet+}$ and $\mathbf{16}^{\bullet+}$ show that these species also consist of two conformers each, which do not equilibrate in the temperature range 200-320 K (ESR, dichloromethane). The interpretation of the superimposed ESR and ENDOR spec-

tra, however, and particularly the assignment of the small coupling constants to the individual conformers is difficult. Probably, only extensive specific deuterations of these compounds could allow a deeper insight to be gained. ENDOR and triple resonance studies of the radical cations in trifluoroacetic acid at 266 K revealed the major splittings of $\mathbf{6}^{\bullet+}$ [conformer A: a(1,3,10,13-H) = +5.43, a(H-OCH_3, 12 H) = +1.34 G; conformer B: a(1,3,10,13-H) = +5.23, a(H-OCH_3, 12 H) = +1.34 G], $\mathbf{11}^{\bullet+}$ [conformer A: a(1,3,10,13-H) = +5.49, a(H-OCH_3, 12 H) = +1.34 G; conformer B: a(1,3,10,13-H) = +5.26, a(H-OCH_3, 12 H) = +1.34 G], and $\mathbf{16}^{\bullet+}$ [conformer A: a(3,10-H) = +7.25, a(H-OCH_3, 6 H) = +2.67 G; conformer B: a(3,10-H) = +6.93, a(H-OCH_3, 6 H) = +2.67 G]. The results obtained prove that a fast intramolecular electron transfer occurs between the two electrophores in $\mathbf{6}^{\bullet+}$ and $\mathbf{11}^{\bullet+}$ owing to the short interplanar distances of ca. 3.3 Å. These observations are in line with the results obtained for the [3.3]paracyclophane radical anion ($\mathbf{2}^{\bullet-}$)[5]. The large β-hydrogen splittings of $\mathbf{6}^{\bullet+}$, $\mathbf{11}^{\bullet+}$ and $\mathbf{16}^{\bullet+}$ point to small dihedral angles θ. This is in agreement with the crystal structures of **6** and **11**, which show dihedral angles of ca. 30°[2b].

In the [4.4]paracyclophane radical cations $\mathbf{7}^{\bullet+}$ and $\mathbf{12}^{\bullet+}$, the interplanar distance between the π-systems is considerably larger. The crystal structure of **7** reveals a distance of 4.01 Å[3]. This increased separation may lead to a significant change in the intramolecular interaction between the electrophores. The ESR spectrum of the *pseudoortho* $\mathbf{12}^{\bullet+}$ exhibits no clear hyperfine structure. In the ENDOR spectrum (Figure 5, top), besides a non-resolved center line, four line pairs are clearly visible corresponding to a(1,4,11,14-H) = +1.77, a(H-OCH_3) = +1.53, a(7,10,17, 20-H) = −0.31, and a(H) = +0.55 G. The splittings were assigned based on general triple resonance[18] (Figure 5, middle), yielding the relative signs, and on special triple resonance[18], which, by comparison of the line intensities, identified the a(H-OCH_3) coupling constant representing twelve hydrogen atoms. The magnitudes of the observed splittings give unambiguous evidence that the electron transfer between the two electrophores in $\mathbf{12}^{\bullet+}$ at 265 K is still fast as compared to the ESR time scale. At lower temperatures (Figure 5, 180 K), however, line broadening of the outer line pairs is observed, which probably indicates that the rate of the intramolecular electron transfer comes close or falls within the range of the ESR time scale.

In contrast to $\mathbf{12}^{\bullet+}$, the isomeric *pseudogeminal* radical cation $\mathbf{7}^{\bullet+}$ gives somewhat different results. The ESR spectrum at 170 K (Figure 6, middle) shows the indicated hyperfine structure of nine lines with a(H) ≈ 2.63 G (8 H), which is supported by simulations. Only at low temperature could weak ENDOR signals (190 K, Figure 6, bottom) be observed, yielding a(4,11-H) = +2.79, a(H-OCH_3) = +2.48 (6H), a(7,10-H) = −0.20, a(H) = +0.90, and a(H) = +0.65 G. The given assignments are again based on general and special triple resonance experiments. All ESR and ENDOR results at low temperature are in accord with a localized radical cation, even if the magnitudes of the splittings are smaller than those of the reference radical cation $\mathbf{17}^{\bullet+}$.

Figure 5. ^{1}H-ENDOR spectrum of the radical cation $\mathbf{12}^{\bullet+}$ in trifluoroacetic acid at 265 K together with a general triple resonance spectrum, pump frequency 12.39 MHz, and ^{1}H-ENDOR spectrum of $\mathbf{12}^{\bullet+}$ in dichloromethane/trifluoroacetic acid (99:1) at 180 K

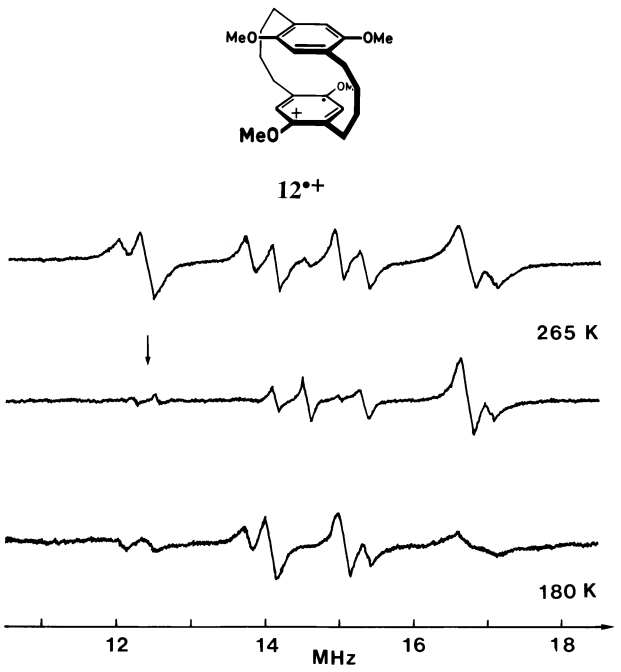

Figure 6. Radical cation $\mathbf{7}^{\bullet+}$ in dichloromethane/trifluoroacetic acid (99:1): ESR spectra at 320 and 170 K, and ^{1}H-ENDOR spectrum at 190 K

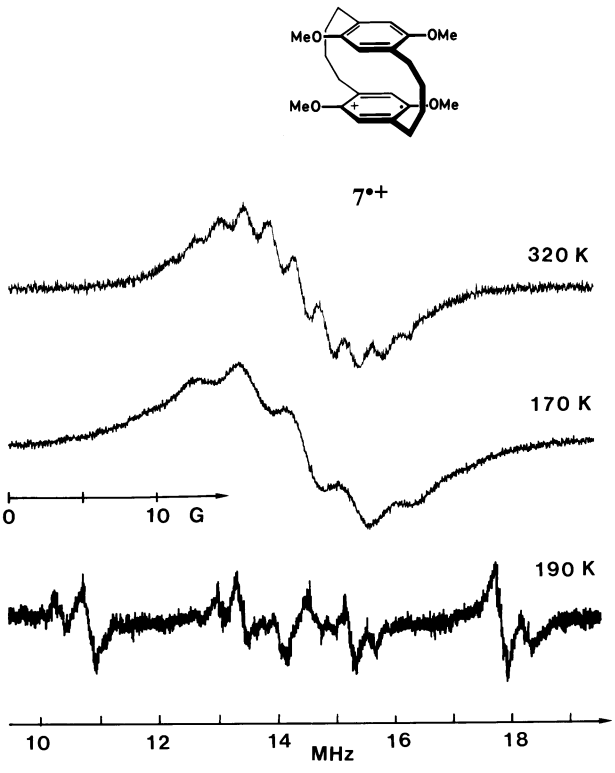

With increasing temperature, the ESR spectrum changes and at ca. 300 K develops the indicated seventeen-line hyperfine structure (Figure 6, top) with a(H) » 1.46 G (12H-

OCH_3 and 1,4,11,14-H). This points to a delocalization of the unpaired electron over both electrophores, i.e. the intramolecular electron exchange becomes faster than the ESR time scale. Unfortunately, the low resolution of the ESR spectra, as well as the relative decrease of the *a*(4,11-H) splitting owing to thermal changes of the tetrahedral angle [orientation of the β-C-H bond with respect to the axis of the adjacent π(2*p*)-orbital] did not allow for a further analysis. The present results suggest that at low temperature $\mathbf{7}^{\bullet+}$ exists in a conformation with maximum separation of the electrophores close to that found in the crystal structure of **7** (4.01 Å[3]). With increasing temperature, the bridges become more and more flexible, thus promoting the intramolecular electron transfer between the electrophores by direct mutual contacts.

Similar results were obtained from the radical cations $\mathbf{8}^{\bullet+}$ and $\mathbf{9}^{\bullet+}$ with further extended bridges. The ESR spectrum of $\mathbf{8}^{\bullet+}$ at 180 K shows the nine-line hyperfine structure corresponding to *a*(5,12-H) = 4.50 and *a*(H-OCH_3) = 3.10 (6 H) evaluated by simulations. Up to 260 K (Figure 7), this nine-line pattern is preserved. However, the magnitude of the splittings decreases considerably [*a*(5,12-H) = 3.30 and *a*(H-OCH_3) = 2.66 G (6 H)], indicating that conformational changes induced by the higher molecular flexibility obstruct a coplanar arrangement of the methoxy groups with respect to the π-plane and changes the dihedral angle of the β-CH_2 hydrogen atoms. At 340 K (Figure 7), the seventeen-line hyperfine structure [*a*(H) ≈ 1.50 G (16 H)] proves that a fast intramolecular electron transfer takes place by mutual collisions of the electrophores. The same is valid for the radical cation $\mathbf{9}^{\bullet+}$. At low temperature (Figure 8), the nine-line hyperfine pattern [220 K: *a*(7,14-H) = 4.13 and *a*(H-OCH_3) = 3.05 G (6 H)] again gives evidence for a localized radical cation, whereas at higher temperatures the indicated seventeen-line hyperfine structure [Figure 8; 290 K: and *a*(H) ≈ 1.50 G (16 H)] points to a delocalization of the unpaired electron over both electrophores, clearly as a result of their mutual collisions.

Conclusions

The results of the cyclic voltammetric measurements and the ESR/ENDOR investigations suggest that the studied paracyclophane radical cations $\mathbf{4}^{\bullet+}-\mathbf{12}^{\bullet+}$ can be divided into two groups with regard to their intramolecular electron exchange. In the [2.2.2.2]-, [2.2]-, and [3.3]paracyclophane radical cations $\mathbf{4}^{\bullet+}-\mathbf{6}^{\bullet+}$, $\mathbf{10}^{\bullet+}$ and $\mathbf{11}^{\bullet+}$, with short interplanar distances (3.05−3.32 Å), there is a strong intramolecular electronic interaction between the two electrophores. This is substantiated by the distinct difference between the first and second oxidation potentials, $\Delta E = E_2^0 - E_1^0 \geq 0.25$ V, and the delocalization of the unpaired electron over both electrophores. The [5.5]- and [7.7]paracyclophane radical cations $\mathbf{8}^{\bullet+}$ and $\mathbf{9}^{\bullet+}$ with $\Delta E < 0.1$ V and interplanar distances ≥ 5.1 Å[4], on the other hand, are localized radical cations at low temperature (ca. 220 K), i.e. the delocalization of the unpaired electron is restricted to one π-moiety. At higher temperatures (ca. 300 K), owing to the growing molecular flexibility, the number of intramolecular contacts (collisions) between the electrophores increases significantly, and intramolecular electron transfer becomes fast on the ESR time scale (ca. 10^7 s^{-1}). Intermedi-

Figure 7. ESR spectra of the radical cation $\mathbf{8}^{\bullet+}$ in trifluoroacetic acid at 340, 293 and 260 K

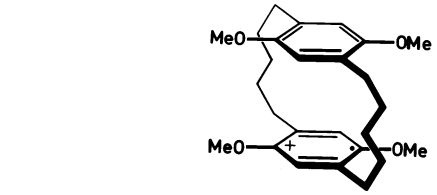

$\mathbf{8}^{\bullet+}$

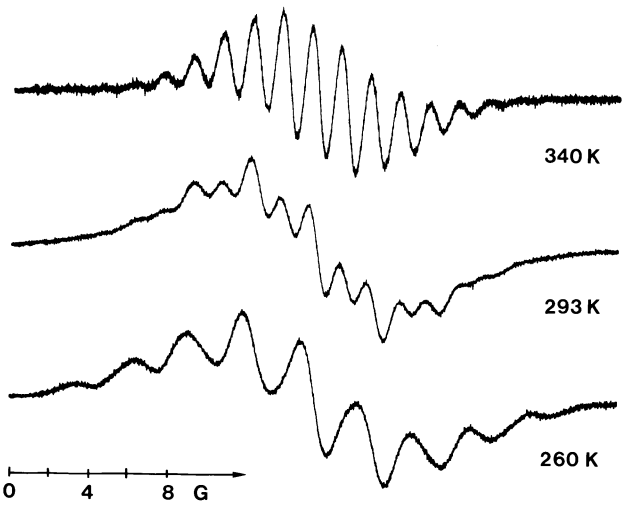

Figure 8. ESR spectra of the radical cation $\mathbf{9}^{\bullet+}$ in dichloromethane/trifluoroacetic acid (99:1) at 290 and 190 K

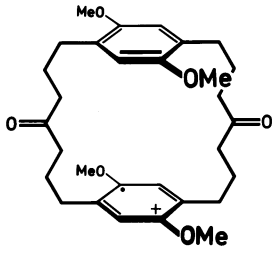

$\mathbf{9}^{\bullet+}$

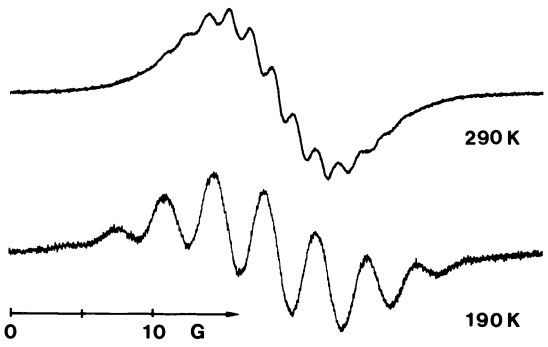

ate or borderline cases are the [4.4]paracyclophane radical cations $\mathbf{7}^{\bullet+}$ and $\mathbf{12}^{\bullet+}$ ($\Delta E = 0.21$ V, interplanar distance ca. 4.0 Å). In such cases, although the difference between the first and second oxidation potentials still indicates some electronic interaction between the electrophores, the required reorganization for the electron transfer, i.e. the planarization of the methoxy groups with respect to the π-plane in the second electrophore, apparently dictates that $\mathbf{7}^{\bullet+}$ and $\mathbf{12}^{\bullet+}$ are basically localized radical cations. Their relatively close interplanar distances, however, facilitate mutual contacts of the electrophores with the consequence that the intramolecular electron transfer at room temperature is fast on the ESR time scale.

Experimental Section

General: Melting points were recorded with a Büchi 510 and are uncorrected. − Analytical TLC: DC Micro Cards Polygram SIL G/UV_{254}, Macherey-Nagel. − ^{1}H NMR: Bruker Physik WP-80, AM 360 or AM 500 (internal reference tetramethylsilane, temperature 305 K). − MS: Finnigan MAT 212 or Jeol JMS-SX 102A (ionization potential 70 eV; only the most prominent peaks are listed, usually with $I_{rel} > 5\%$). − Cyclic voltammetry: All electrochemical studies were performed using an EG & G Princeton Applied Research 263 A potentiostat attached to an EG & G electrochemical microcell K0264, which was equipped with a glassy carbon millielectrode (G0229, 2 mm diameter) as working electrode, a standard Ag/AgCl reference electrode (K0265), and a platinum wire counterelectrode (K0226). The measurements were carried out on degassed anhydrous acetonitrile solutions containing the sample (0.5−1 mM) and tetrabutylammonium hexafluorophosphate (0.1 M) as supporting electrolyte at 298 K. Cyclic voltammograms were scanned at a sweep rate of ca. 100 mV s^{-1}. Redox potentials are referred to ferrocene ($FeCp_2$, $E_1^0 = +0.352$ V) set to 0 V. − ESR and ENDOR: Bruker ESP 300 spectrometer equipped with the ER 252 (ENMR) ENDOR system; *g* values were determined using an NMR Gauss meter and a Hewlett-Packard 5342A microwave frequency counter; this was calibrated with the perylene radical cation. Hyperfine coupling constants measured in MHz (ENDOR) were converted into Gauss using 1 MHz = ($0.7145/g_{ex}$) G. − The radical cations $\mathbf{4}^{\bullet+}$−$\mathbf{17}^{\bullet+}$ were generated in trifluoroacetic acid (99.7% for protein sequencing, Merck) or in dichloromethane (99.9%, HPLC grade, Aldrich)/trifluoroacetic acid (99:1) by oxidation of the parent compounds with little lead tetraacetate dissolved in trifluoroacetic acid.

The compounds 4,7,12,15-tetramethoxy[2.2.2.2]paracyclophane (**4**)[21], *pseudogeminal* (**5**)[1b][1c] and *pseudoortho* 4,7,12,15-tetramethoxy[2.2]paracyclophane (**10**)[1a][1c], *pseudogeminal* (**6**)[2a][2b] and *pseudoortho* 5,8,14,17-tetramethoxy[3.3]paracyclophane (**11**)[2a][2b], *pseudogeminal* (**7**)[3] and *pseudoortho* 6,9,16,19-tetramethoxy[4.4]paracyclophane (**12**)[3], *pseudogeminal* 7,10,18,21-tetramethoxy[5.5]paracyclophane (**8**)[4], 9,12,22,25-tetramethoxy[7.7]paracyclophane-4,17-dione (**9**)[16], and 4,7-dimethoxy[2.2]paracyclophane (**15**)[22] were available in our laboratory or were prepared as described in the literature.

1,4-Bis(hydroxy[D_2]methyl)-2,5-dimethoxybenzene: To a stirred suspension of lithium aluminium deuteride (7.0 g, 0.17 mol) in anhydrous tetrahydrofuran (200 ml), a solution of dimethyl 2,5-dimethoxyterephthalate (38.1 g, 0.15 mol) in anhydrous tetrahydrofuran (300 ml) was added over a period of 30 min at such a rate that the mixture boiled gently. Heating to reflux was continued for 1 h. After addition of ethyl acetate (10 ml) and 2 N H_2SO_4 (30 ml) at room temperature, the mixture was filtered and the residue was washed with tetrahydrofuran. The combined filtrates were concentrated under reduced pressure. Crystallization of the residue from water afforded 1,4-bis(hydroxy[D_2]methyl)-2,5-dimethoxybenzene (21 g, 69%) as colorless needles, m.p. 161−162 °C (m.p. of the non-deuterated compound 164−165 °C[23]). − ^{1}H NMR (80 MHz, [D_6]DMSO): δ = 3.72 (s, 6 H, OCH_3), 4.75 (s, 2 H, OH), 7.01 (s, 2 H, 3,6-H). − EI-MS; *m/z*: 202 [$M^{\bullet+}$].

1,4-Bis(chloro[D_2]methyl)-2,5-dimethoxybenzene: Thionyl chloride (16 ml, 0.22 mol) was added dropwise to a stirred suspension of 1,4-bis(hydroxy[D_2]methyl)-2,5-dimethoxybenzene (20.2 g, 0.10 mol) in dichloromethane (300 ml). A few minutes after the starting material had dissolved, the product precipitated. The mixture was then stirred for a further 1 h. After cooling to −80 °C, the product was collected and recrystallized from acetone to give 1,4-bis(chloro-[D_2]methyl)-2,5-dimethoxybenzene (19.0 g, 79%) as colorless crystals, m.p. 163−164 °C (m.p. of the non-deuterated compound 167.5 °C[24]). − ^{1}H NMR (80 MHz, $CDCl_3$): δ = 3.85 (s, 6 H, OCH_3), 6.93 (s, 2 H, 3,6-H). − EI-MS; *m/z*: 242, 240, 238 [$M^{\bullet+}$].

1,4-Bis(mercapto[D_2]methyl)-2,5-dimethoxybenzene: Prepared from 1,4-bis(chloro[D_2]methyl)-2,5-dimethoxybenzene and thiourea as described in the literature for the non-deuterated compound[25], m.p. 110−111 °C (m.p. of the non-deuterated compound 111−113 °C[25]). − ^{1}H NMR (80 MHz, $CDCl_3$): δ = 1.91 (s, 2 H, SH), 3.85 (s, 6 H, OCH_3), 6.82 (s, 2 H, 3,6-H). − EI-MS; *m/z*: 234 [$M^{\bullet+}$].

1,4-Bis(chloro[D_2]methyl)[D_4]benzene: Prepared from [D_6]benzene, [D_2]paraformaldehyde and thionyl chloride as described in the literature for the non-deuterated compound[26], m.p. 99−100 °C (m.p. of the non-deuterated compound 100 °C[26]). − EI-MS; *m/z*: 246, 244, 242 [$M^{\bullet+}$].

4,7-Dimethoxy[1,1,10,10,12,13,15,16-D_8][2.2]paracyclophane (**15a**): Prepared from 1,4-bis(mercaptomethyl)-2,5-dimethoxybenzene and 1,4-bis(chloro[D_2]methyl)[D_4]benzene according to procedures described in the literature for the non-deuterated compound[27], m.p. 185−186 °C (m.p. of the non-deuterated compound 181−182 °C[22]). − ^{1}H NMR (500 MHz, $CDCl_3$): δ = 2.51 (d, ^2J = 13.1 Hz, 2 H, 2,9-*syn*-H with regard to 5,8-H), 3.40 (d, 2 H, 2,9-*anti*-H with regard to 5,8-H), 3.70 (s, 6 H, OCH_3), 5.73 (s, 2 H, 5,8-H); irradiation of the 5,8-H signal at δ = 5.73 yielded a positive NOE response for OCH_3 at δ = 3.70 and for 2,9-H at δ = 2.51. − EI-MS; *m/z* (%): 277 (11), 276 (58) [$M^{\bullet+}$], 165 (13), 164 (100) [$M^{\bullet+}$ − C_8D_8], 134 (28), 91 (14).

4,7-Dimethoxy[1,1,2,2,9,9,10,10,12,13,15,16-D_{12}][2.2]paracyclophane (**15b**): Prepared from 1,4-bis(mercapto[D_2]methyl)-2,5-dimethoxybenzene and 1,4-bis(chloro[D_2]methyl)[D_4]benzene as described above, m.p. 185−186 °C. − ^{1}H NMR (500 MHz, $CDCl_3$): δ = 3.70 (s, 6 H, OCH_3), 5.73 (s, 2 H, 5,8-H). − EI-MS; *m/z* (%): 281 (12), 280 (61) [$M^{\bullet+}$], 169 (13), 168 (100) [$M^{\bullet+}$ − C_8D_8], 167 (13), 138 (35), 112 (13).

6,9-Dimethoxy-3,12-dithia[4.4]paracyclophane: To a boiling, stirred suspension of potassium carbonate (25 g) in ethanol/water (95:5, 3 l) a solution containing 1,4-bis(2-bromoethyl)benzene (10.2 g, 35 mmol) and 1,4-bis(mercaptomethyl)-2,5-dimethoxybenzene (8.06 g, 35 mmol) in toluene (250 ml) was added dropwise over a period of 5 h. After cooling, the mixture was filtered and the filtrate was concentrated under reduced pressure. Chromatography of the residue on silica gel using cyclohexane/toluene (1:1) as eluent afforded 6,9-dimethoxy-3,12-dithia[4.4]paracyclophane (5.9 g, 47%) as colorless crystals from ethyl acetate/ethanol, m.p. 142−143 °C. − EI-MS; *m/z* (%): 360 (100) [$M^{\bullet+}$], 197 (7), 165 (23), 164 (22). −

$C_{20}H_{24}O_2S_2$ (360.5): calcd. C 66.63, H 6.71; found C 66.77, H 6.85.

6,9-Dimethoxy-3,12-dithia[4.4]paracyclophane 3,3,12,12-Tetraoxide: To a vigorously stirred solution of 6,9-dimethoxy-3,12-dithia[4.4]paracyclophane (5.41 g, 15 mmol) in dichloromethane (250 ml), 50−60% 3-chloroperoxybenzoic acid (25 g, ca. 75 mmol) was added in small portions over a period of 10 min. Stirring at room temperature was continued for 10 h. The precipitated product was filtered and recrystallized from dimethyl sulfoxide to give 6,9-dimethoxy-3,12-dithia[4.4]paracyclophane 3,3,12,12-tetraoxide (2.1 g, 30%) as colorless crystals, m.p. 342−343 °C (dec.). − $C_{20}H_{24}O_6S_2$ (424.5): calcd. C 56.58, H 5.70; found C 56.45, H 5.88.

5,8-Dimethoxy[3.3]paracyclophane (**16**): 6,9-Dimethoxy-3,12-dithia[4.4]paracyclophane 3,3,12,12-tetraoxide (2.0 g, 4.7 mmol) was pyrolyzed in portions of 400 mg at 600 °C/10^{-4} Torr (evaporation temperature 350 °C) according to procedures described in the literature[3][28]. Chromatography of the pyrolysis product on silica gel using toluene/dichloromethane (9:1) as eluent afforded compound **16** (390 mg, 28%; R_f = 0.70, dichloromethane) as colorless crystals from ethanol, m.p. 132−133 °C (ref.[29]: m.p. 131.5−132 °C). − ^{1}H NMR (500 MHz, $CDCl_2CDCl_2$ at 363 K to achieve equilibration of the chair and boat conformers): δ = 1.90−2.05 (m, 2 H, CH_2), 2.25−2.45 (m, 4 H, CH_2), 2.65−2.85 (m, 4 H, CH_2), 3.05−3.20 (m, 2 H, CH_2), 3.81 (s, 6 H, OCH_3), 6.19 (s, 2 H, 6,9-H), 6.71 (d, ^3J = 8.1 Hz, 2 H, 14,17- or 15,18-H), 6.91 (d, 2 H, 15,18- or 14,17-H). − EI-MS; *m/z* (%): 297 (81), 296 (100) [$M^{\bullet+}$], 177 (14), 165 (18), 151 (30), 131 (14), 117 (26), 91 (25). − $C_{20}H_{24}O_2$ (296.4): calcd. C 81.04, H 8.16; found C 81.19, H 8.14.

7,10-Dimethoxy-2,15-dithia[5.5]paracyclophane: To a boiling, stirred solution of potassium hydroxide (4.0 g, 71 mmol) in methanol p.a. (1.9 l) and tetrahydrofuran p.a. (100 ml) under argon, a solution of 1,4-bis(3-bromopropyl)-2,5-dimethoxybenzene (3.82 g, 10 mmol), 1,4-bis(mercaptomethyl)benzene (1.70 g, 10 mmol) and 2 N acetic acid (0.3 ml) in tetrahydrofuran p.a./methanol p.a. (1:1, 800 ml) was added dropwise over a period of 8 h. Heating under reflux was continued for a further 1 h. After cooling and addition of 2 N hydrochloric acid (25 ml), the solvent was distilled off under reduced pressure. After addition of water (400 ml), the residue was extracted with dichloromethane (4 × 250 ml). The combined extracts were dried ($MgSO_4$) and concentrated under reduced pressure. Flash chromatography [silica gel (35−70 mm, Amico), toluene/chloroform, 1:1] of the residue afforded 7,10-dimethoxy-2,15-dithia[5.5]paracyclophane (2.28 g, 59%; R_f = 0.49, dichloromethane) as colorless crystals from ethanol, m.p. 126−127 °C. − ^{1}H NMR (360 MHz, $CDCl_3$): δ = 1.65−2.35 (m, 10 H, CH_2), 3.00−3.15 (m, 2 H, CH_2), 3.58 (s, 4 H, 1,1,16,16-H), 3.75 (s, 6 H, OCH_3), 6.47 (s, 2 H, 8,11-H), 7.03 (s, 4 H, 18,19,21,22-H). − EI-MS; *m/z* (%): 390 (12), 389 (28), 388 (100) [$M^{\bullet+}$], 284 (26), 237 (13), 209 (11), 177 (20), 105 (55), 104 (22), 91 (20). − $C_{22}H_{28}O_2S_2$ (388.6): calcd. C 68.00, H 7.26, S 16.50; found C 67.98, H 7.29, S 16.69.

7,10-Dimethoxy-2,15-dithia[5.5]paracyclophane 2,2,15,15-Tetraoxide: To a vigorously stirred solution of 7,10-dimethoxy-2,15-dithia[5.5]paracyclophane (505 mg, 1.3 mmol) in dichloromethane (75 ml), 50−60% 3-chloroperoxybenzoic acid (2.1 g, ca. 6.5 mmol) was added in small portions over a period of 10 min. Stirring at room temperature was continued for 10 h. Then, dichloromethane (75 ml) and 0.5 M aqueous NaOH (50 ml) were added, and the mixture was stirred for a further 1 h. The organic phase was separated, and the aqueous phase was extracted with dichloromethane (75 ml). The combined organic phases were dried ($MgSO_4$) and concentrated under reduced pressure. Crystallization of the residue from acetone afforded 7,10-dimethoxy-2,15-dithia[5.5]paracyclophane 2,2,15,15-tetraoxide (475 mg, 81%; R_f = 0.53, ethyl acetate) as colorless crystals, m.p. 264−265 °C (dec.). − ^{1}H NMR (360 MHz, $CDCl_3$): δ = 1.95−2.55 (m, 10 H, CH_2), 3.05−3.20 (m, 2 H, CH_2), 3.76 (s, 6 H, OCH_3), 4.13 (s, 4 H, 1,1,16,16-H), 6.52 (s, 2 H, 8,11-H), 7.26 (s, 4 H, 18,19,21,22-H). − EI-MS; *m/z* (%): 454 (15), 453 (24), 452 (100) [$M^{\bullet+}$], 191 (14), 177 (11), 164 (53), 134 (15), 105 (19), 104 (23), 91 (12). − $C_{22}H_{28}O_6S_2$ (452.6): calcd. C 58.38, H 6.24, S 14.17; found C 58.13, H 6.21, S 13.91.

6,9-Dimethoxy[4.4]paracyclophane (**17**): 7,10-Dimethoxy-2,15-dithia[5.5]paracyclophane 2,2,15,15-tetraoxide (4.53 g, 10 mmol) was pyrolyzed in portions of 400 mg at 600 °C/10^{-4} Torr (evaporation temperature 270 °C) according to procedures described in the literature[3][28]. Flash chromatography [silica gel (35−70 mm, Amico), toluene/chloroform, 3:1] afforded compound **17** (1.04 g, 32%; R_f = 0.51, dichloromethane) as colorless crystals from acetone, m.p. 153−154 °C. − ^{1}H NMR (360 MHz, $CDCl_3$): δ = 1.25−2.95 (m, 16 H, CH_2), 3.71 (s, 6 H, OCH_3), 6.24 (s, 2 H, 7,10-H), 6.60−6.85 (m, 4 H, 16,17,19,20-H). − EI-MS; *m/z* (%): 325 (15), 324 (100) [$M^{\bullet+}$], 164 (7), 151 (5), 91 (6). − $C_{22}H_{28}O_2$ (324.5): calcd. C 81.44, H 8.70; found C 81.15, H 8.76.

Pseudogeminal 4,7,12,15-Tetramethoxy[5,8-D_2][2.2]paracyclophane (**5a**): To a stirred solution of 4,7-dibromo-5,8,12,15-tetramethoxy[2.2]paracyclophane (diastereomer m.p. 157−159 °C)[1b][1c] (486 mg, 1 mmol) in anhydrous diethyl ether (50 ml) under argon at −70 °C, a solution of 1.6 M butyllithium in hexane (5 ml, 8 mmol) was added dropwise. After warming to room temperature, stirring was continued for a further 3 h. Then, the mixture was hydrolyzed by adding deuterium oxide (1 ml) and filtered. The residue was extracted with chloroform (50 ml) and the combined extracts were dried (Na_2SO_4) and concentrated. Crystallization of the product from chloroform/pentane afforded compound **5a** (270 mg, 82%) as colorless crystals, m.p. 229−230 °C (m.p. of the non-deuterated compound 229−230 °C[1b][1c]). − ^{1}H NMR (360 MHz, $CDCl_3$): δ = 2.59−2.64 (m, 4 H, 1,2,9,10-*syn*-H with regard to 5,8,13,16-H), 3.44−3.53 (m, 1,2,9,10-*anti*-H with regard to 5,8,13,16-H), 3.64 (s, 6 H, OCH_3), 5.87 (s, 2 H, 13,16-H); irradiation of the 13,16-H signal at δ = 5.87 yielded a positive NOE response for OCH_3 at δ = 3.64 and for 1,2,9,10-H at δ = 2.59−2.64. − EI-MS; *m/z* (%): 331 (23), 330 (92) [$M^{\bullet+}$], 329 (37), 166 (70), 165 (60), 164 (100), 136 (16), 135 (15), 134 (20).

Pseudoortho 4,7,12,15-Tetramethoxy[5,8-D_2][2.2]paracyclophane (**10a**): Prepared as described above using 4,7-dibromo-5,8,12,15-tetramethoxy[2.2]paracyclophane (diastereomer m.p. 137−139 °C)[1b][1c]: Colorless crystals from pentane, m.p. 121−123 °C (m.p. of the non-deuterated compound 121−123 °C[1]). − ^{1}H NMR (360 MHz, $CDCl_3$): δ = 2.58−2.68 (m, 4 H, 1,2,9,10-*syn*-H with regard to 5,8,13,16-H), 3.15−3.24 (m, 1,2,9,10-*anti*-H with regard to 5,8,13,16-H), 3.66 (s, 6 H, OCH_3), 6.10 (s, 2 H, 13,16-H); irradiation of the 13,16-H signal at δ = 6.10 yielded a positive NOE response for OCH_3 at δ = 3.66 and for 1,2,9,10-H at δ = 2.58−2.68. − EI-MS; *m/z* (%): 331 (23), 330 (78) [$M^{\bullet+}$], 329 (36), 166 (62), 165 (60), 164 (100), 136 (14), 135 (15), 134 (18).

[1] [1a] W. Rebafka, H. A. Staab, *Angew. Chem.* **1973**, *85*, 831−832; *Angew. Chem. Int. Ed. Engl.* **1973**, *12*, 776−777. − [1b] W. Rebafka, H. A. Staab, *Angew.Chem.* **1974**, *86*, 234−235; *Angew. Chem. Int. Ed. Engl.* **1974**, *13*, 203−204. − [1c] H. A. Staab, W. Rebafka, *Chem. Ber.* **1977**, *110*, 3333−3350.

[2] [2a] H. A. Staab, C. P. Herz, *Angew. Chem.* **1977**, *89*, 839−840, *Angew. Chem. Int. Ed. Engl.* **1977**, *16*, 799−800. − [2b] H. A. Staab, C. P. Herz, C. Krieger, M. Rentea, *Chem. Ber.* **1983**, *116*, 3813−3830.

[3] H. A. Staab, A. Döhling, C. Krieger, *Liebigs Ann. Chem.* **1981**, 1052−1064.

[4] H. A. Staab, B. Starker, C. Krieger, *Chem. Ber.* **1983**, *116*, 3831−3845.
[5] F. Gerson, W. B. Martin, *J. Am. Chem. Soc.* **1969**, *91*, 1883−1891.
[6] F. Gerson, *Top. Curr. Chem.* **1983**, *115*, 57−105.
[7] J. E. Harriman, A. H. Maki, *J. Chem. Phys.* **1963**, *39*, 778−786.
[8] B. Becker, A. Bohnen, M. Ehrenfreund, W. Wohlfahrt, Y. Sakata, W. Huber, K. Müllen, *J. Am. Chem. Soc.* **1991**, *113*, 1121−1127, and references therein.
[9] F. Gerson, W. Huber, W. B. Martin, P. Caluwe, T. Pepper, M. Szwarc, *Helv. Chim. Acta* **1984**, *67*, 416−424.
[10] K. Shimada, M. Szwarc, *Chem. Phys. Lett.* **1974**, *28*, 540−545.
[11] F. Gerson, T. Wellauer, A. M. Oliver, M. N. Paddon-Row, *Helv. Chim. Acta* **1990**, *73*, 1586−1601.
[12] K. Shimada, G. Moshuk, H. D. Connor, P. Caluwe, M. Szwarc, *Chem. Phys. Lett.* **1972**, *14*, 396−401.
[13] S. F. Rak, L. L. Miller, *J. Am. Chem. Soc.* **1992**, *114*, 1388−1394.
[14] The oxidation potentials of **5**, **6**, **10**, **11**, **13** and **15** in acetonitrile/0.1 M tetrabutylammonium perchlorate have been measured previously using a mercury electrode versus $Ag/AgNO_3$. The data obtained and particularly the relative differences are consistent with the results given in Table 1. T. Geiger, Dissertation, Universität Heidelberg, **1978**.
[15] C. Krieger, unpublished results.
[16] H. A. Staab, G. Matzke, C. Krieger, *Chem. Ber.* **1987**, *120*, 89−91.
[17] W. F. Forbes, P. D. Sullivan, *J. Chem. Phys.* **1968**, *48*, 1411−1413.
[18] H. Kurreck, B. Kirste, W. Lubitz, *Angew. Chem.* **1984**, *96*, 171−193, *Angew. Chem., Int. Ed. Engl.* **1984**, *23*, 173−195, and references given therein.
[19] W. F. Forbes, P. D. Sullivan, *J. Chem. Phys.* **1968**, *48*, 1411−1413; $\mathbf{14}^{\bullet+}$ generated in nitromethane: $a(H\text{-}OCH_3)$ = 2.76 (6 H), $a(H\text{-}CH_3)$ = 2.11 G (12 H).
[20] [20a] R. Benn, N. E. Blank, M. W. Haenel, J. Klein, A. R. Koray, K. Weidenhammer, M. L. Ziegler, *Angew. Chem.* **1980**, *92*, 45−46, *Angew. Chem. Int. Ed. Engl.* **1980**, *19*, 44−45. − [20b] F. A. L. Anet, M. A. Brown, *J. Am. Chem. Soc.* **1969**, *91*, 2389−2391.
[21] H. A. Staab, V. Schwendemann, *Angew. Chem.* **1978**, *90*, 805−807; *Angew. Chem. Int. Ed. Engl.* **1978**, *17*, 756−757. H. A. Staab, V. Schwendemann, *Liebigs Ann. Chem.* **1979**, 1258−1269.
[22] H. A. Staab, V. Taglieber, *Chem. Ber.* **1977**, *110*, 3366−3376.
[23] J. N. Marx, P.-S. Song, P. K. Chui, *J. Heterocycl. Chem.* **1975**, *12*, 417−419.
[24] J. H. Wood, R. E. Gibson, *J. Am. Chem. Soc.* **1949**, *71*, 393−395.
[25] Henkel and Cie, GmbH, Brit. Pat. 807,720, **1959** [*Chem. Abstr.* **1960**, *54*, 412g].
[26] R. Stroh, W. Hahn, *Methoden Org. Chem. (Houben-Weyl) 4th ed.* **1962**, vol. V/3, p. 1002.
[27] M. Takeshita, H. Tsuzuki, M. Tashiro, *Bull. Chem. Soc. Jpn.* **1992**, *65*, 2076−2082.
[28] H. A. Staab, M. W. Haenel, *Chem. Ber.* **1973**, *106*, 2190−2202.
[29] T. Shinmyozu, T. Inazu, T. Yoshino, *Chem. Lett.* **1977**, 1347−1350.

[97226]